Microwave-Induced Auditory Effect in a Dielectric Sphere

NIKOLAOS K. UZUNOGLU, MEMBER, IEEE, AND SPYRIDON I. POLYCHRONOPOULOS

Abstract —The acoustic pressure wave generation inside an electromagnetically lossy dielectric sphere from an incident microwave pulse is analyzed rigorously. The pressure wave equation, derived by using the first-order approximation of a thorough formulation on microwave-induced thermoacoustic effect in dielectrics, is employed. The inhomogeneous hyperbolic type pressure wave differential equation is solved by employing a Green's function theory approach. The inhomogeneous term of this equation is proportional to the time derivative of the absorbed power ($\mathbb{P}$) per unit volume inside the sphere. The boundary conditions on the dielectric sphere–air interface are taken into account. The power $\mathbb{P}$ is computed by applying the exact Mie theory solution for the dielectric sphere. Two types of acoustic waves are derived inside the sphere: a) a transient burst type pressure wave, corresponding to the free-space contribution of Green's function, and b) an infinite set of damped oscillations related to the normal acoustic modes of the spherical resonator. Numerical results are computed and presented for several cases.

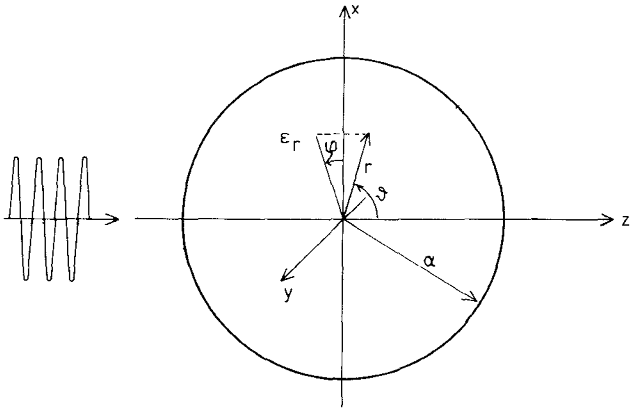

Fig. 1 Illumination of a dielectric sphere from a microwave pulse.

I. INTRODUCTION

MICROWAVE pulses impinging on the heads of mammalian animals and humans have been shown to generate audible sounds [1]–[4]. It has been shown that a conventional bone conduction mechanism is involved in sensing microwave pulses [5]–[7].

Several physical processes such as radiation pressure, electrostriction, and thermal expansion have been proposed in the past to explain the hearing of microwave pulses [7]–[10]. Among these phenomena the thermoelastic expansion mechanism has found wide acceptance [11]–[13].

Recently the microwave-induced thermoacoustic effect in dielectrics and its coupling to external media has been analyzed by applying a thorough thermodynamical formulation [14]. Highly nonlinear differential equations have been derived in the general case. Assuming small amplitude waves and isotropic acoustic properties of the dielectric medium, the fundamental equations describing the coupling between electromagnetic and acoustic waves have been simplified considerably and linear equations have been obtained [14]. In the present paper the linear pressure wave equation is solved by applying a Green's function approach when an arbitrary sphere of arbitrary size is illuminated by a microwave pulse. In this context the dielectric sphere is taken to be homogeneous in terms of the electromagnetic and acoustic properties. The proposed solution furnishes results that can be interpreted easily. It is shown that two types of acoustic waves are generated, corresponding to a free-space transient acoustic pulse and an infinite summation of excited spherical cavity damped normal mode waves similar to those of [12] and [13].

Manuscript received December 5, 1987; revised April 18, 1988.
The authors are with the Department of Electrical Engineering, National Technical University of Athens, Athens 106 82, Greece.
IEEE Log Number 8822910.

II. FORMULATION OF THE ACOUSTIC FIELD BOUNDARY VALUE PROBLEM

In Fig. 1 the geometry of the dielectric sphere illuminated from a microwave pulse is given. The dielectric sphere electromagnetic properties are defined in terms of the complex relative permittivity ϵ_r while the whole space is assumed to be nonmagnetic, with $\mu = \mu_0 \cong 4\pi \times 10^{-7}$ (H/m) being the free-space permeability. The free-space (air region) permittivity is $\epsilon = \epsilon_0 \cong 10^{-9}/(36\pi)$ (F/m). The radius of the dielectric sphere α is taken to be arbitrary in comparison with the incident wave free-space wavelength λ.

Following the [14, eq. (28)], the pressure field $p = p(\boldsymbol{r}, t)$ induced inside and outside of the dielectric sphere satisfies the wave equation

$$\left(\frac{\partial^2}{\partial t^2} - c^2(\boldsymbol{r})\nabla^2\right)p(\boldsymbol{r}, t) = C_0 \frac{\partial \mathbb{P}(r, t)}{\partial t} \tag{1}$$

where $c(\boldsymbol{r})$ is the velocity of the acoustic waves and, because of the spherical geometry,

$$c(r) = \begin{cases} c_1 & \text{for } r < \alpha \\ c_2 & \text{for } r > \alpha \end{cases} \tag{2}$$

where c_1 and c_2 are the acoustic wave velocities inside the dielectric sphere and air regions, respectively. The right-hand side of (1) is the source term and $\mathbb{P}(\boldsymbol{r}, t)$ is the average electromagnetic power converted into heat per unit volume (W/m^3) inside the material medium. The losses inside the air region are neglible and therefore $\mathbb{P} = 0$ for $r > \alpha$. In order to compute the power density $\mathbb{P}$ for $r < \alpha$, the full-wave solution of the scattering of a plane electromagnetic wave is employed in Section IV of this paper. The proportionality constant C_0 appearing in the right-hand side of (1) is related to the thermodynamic quantities of the dielectric sphere and is given in [14]. In addition to (1), the pressure field $p(\boldsymbol{r}, t)$ on the $r = \alpha$ discontinuity spherical surface should satisfy the following boundary conditions (see [14, eq. (31)]:

$$p(\boldsymbol{r}, t)|_{r=\alpha-} = p(\boldsymbol{r}, t)|_{r=\alpha+} \tag{3}$$

$$\frac{1}{\rho_{10}} \frac{\partial p(\boldsymbol{r}, t)}{\partial r}\bigg|_{r=\alpha-} = \frac{1}{\rho_{20}} \frac{\partial p(\boldsymbol{r}, t)}{\partial r}\bigg|_{r=\alpha+} \tag{4}$$

where ρ_{10} and ρ_{20} are the average mass densities of the dielectric and air media, respectively.

In order to determine the pressure $p(\boldsymbol{r}, t)$, a Green's function approach will be employed. To this end, (1) is rewritten as follows:

$$\left(\nabla^2 - \frac{1}{c^2(r)} \frac{\partial^2}{\partial t^2}\right) p(\boldsymbol{r}, t) = -V(\boldsymbol{r}, t) \tag{5}$$

where

$$V(\boldsymbol{r}, t) = \frac{C_0}{c^2(r)} \frac{\partial \mathbb{P}(\boldsymbol{r}, t)}{\partial t}. \tag{6}$$

The associated Green's function $G(\boldsymbol{r}, r'/t - t')$ is required to satisfy the differential equation

$$\left(\nabla^2 - \frac{1}{c^2(r)} \frac{\partial^2}{\partial t^2}\right) G(\boldsymbol{r}, r'/t - t') = -\delta(\boldsymbol{r} - \boldsymbol{r}')\delta(t - t') \tag{7}$$

and, according to the causality principle,

$$G(\boldsymbol{r}, r'/t - t') = 0 \qquad \text{for } t < t'. \tag{8}$$

In physical terms $G(\boldsymbol{r}, \boldsymbol{r}'/t - t')$ is the acoustic response observed at the point $\boldsymbol{r}$ and the instant t for an elementary excitation at the point $\boldsymbol{r}'$ occurring at the instant $t' < t$.

The boundary conditions to be satisfied on the $r = \alpha$ spherical surface by the $G(\boldsymbol{r}, \boldsymbol{r}'/t - t')$ function will be specified in the course of the analysis. In order to proceed with the solution of (5), Fourier transformations of (5) and (6) are taken along the t time axis. Then,

$$(\nabla^2 + \kappa^2(r)) p_\omega(\boldsymbol{r}) = -V_\omega(\boldsymbol{r}) \tag{9}$$

$$(\nabla^2 + \kappa^2(r)) G_\omega(\boldsymbol{r}, \boldsymbol{r}') = -\delta(\boldsymbol{r} - \boldsymbol{r}') \tag{10}$$

where

$$\kappa(r) = \omega / c(r) \tag{11}$$

$$\begin{pmatrix} p_\omega(\boldsymbol{r}) \\ G_\omega(\boldsymbol{r}, \boldsymbol{r}') \end{pmatrix} = F\begin{pmatrix} p(\boldsymbol{r}, t) \\ G(\boldsymbol{r}, \boldsymbol{r}'/t) \end{pmatrix} = \int_{-\infty}^{+\infty} dt \begin{pmatrix} p(\boldsymbol{r}, t) \\ G(\boldsymbol{r}, \boldsymbol{r}'/t) \end{pmatrix} e^{-j\omega t}. \tag{12}$$

The corresponding inverse Fourier transformations are written easily as follows:

$$\begin{pmatrix} p(\boldsymbol{r}, \tau) \\ G(\boldsymbol{r}, \boldsymbol{r}'/\tau) \end{pmatrix} = F^{-1}\begin{pmatrix} p_\omega(\boldsymbol{r}) \\ G_\omega(\boldsymbol{r}, \boldsymbol{r}') \end{pmatrix} = \frac{1}{2\pi} \int_{-\infty}^{+\infty} d\omega \begin{pmatrix} p_\omega(\boldsymbol{r}) \\ G_\omega(\boldsymbol{r}, \boldsymbol{r}') \end{pmatrix} e^{+j\omega\tau}. \tag{13}$$

Assuming the Green's function $G_\omega(\boldsymbol{r}, \boldsymbol{r}')$ is known, the fundamental wave equation (9) can be solved. To this end, according to Green's theorem,

$$\iiint_V d\boldsymbol{r}' \left(p_\omega(\boldsymbol{r}') \nabla^2 G_\omega(\boldsymbol{r}, \boldsymbol{r}') - G_\omega(\boldsymbol{r}, \boldsymbol{r}') \nabla^2 p_\omega(\boldsymbol{r}') \right) = \iint_S dS_R \hat{n} \cdot \left(p_\omega(\boldsymbol{R}) \nabla G_\omega(\boldsymbol{r}, \boldsymbol{R}) - G_\omega(\boldsymbol{r}, \boldsymbol{R}) \nabla p_\omega(\boldsymbol{R}) \right) \tag{14}$$

where V is a volume enclosed inside a closed surface S, $\boldsymbol{R}$ is the position vector, and $\hat{n}$ is the outward unit vector on the surface S. The function $p_\omega(\boldsymbol{r}')$ and $G_\omega(\boldsymbol{r}, \boldsymbol{r}')$ and their first derivatives should be continuous inside the volume V. Applying (14) separately for the cases when V is the spherical volume of the dielectric medium and the infinite air region, using the radiation condition for $|\boldsymbol{R}| \to +\infty$, substituting (9) and (10), and adding the two integrals, the following relation is derived:

$$\begin{aligned} -p_\omega(\boldsymbol{r}) + \iiint_{V(r' < \alpha)} d\boldsymbol{r}' G_\omega(\boldsymbol{r}, \boldsymbol{r}') V_\omega(\boldsymbol{r}') = \iint_{S(r' = \alpha)} ds_R \Bigg(p_\omega(\boldsymbol{r}') \Bigg(\frac{\partial G_\omega(\boldsymbol{r}, \boldsymbol{r}')}{\partial r'}\bigg|_{r'=\alpha-} - \frac{\partial G_\omega(\boldsymbol{r}, \boldsymbol{r}')}{\partial r'}\bigg|_{r'=\alpha+} \Bigg) - \Bigg(G_\omega(\boldsymbol{r}, \boldsymbol{r}') \frac{\partial p(\boldsymbol{r}')}{\partial r'}\bigg|_{r'=\alpha-} \\ - G_\omega(\boldsymbol{r}, \boldsymbol{r}') \frac{\partial p(\boldsymbol{r}')}{\partial r'}\bigg|_{r'=\alpha+} \Bigg) \Bigg). \end{aligned} \tag{15}$$

If now, the boundary conditions to be satisfied at $r' = \alpha$ by the Green's function are chosen such that

$$\frac{\partial G_\omega(\boldsymbol{r}, \boldsymbol{r}')}{\partial r'}\bigg|_{r'=\alpha-} = \frac{\partial G_\omega(\boldsymbol{r}, \boldsymbol{r}')}{\partial r'}\bigg|_{r'=\alpha+} \tag{16}$$

$$\rho_{10} G_\omega(\boldsymbol{r}, \boldsymbol{r}')|_{r'=\alpha-} = \rho_{20} G_\omega(\boldsymbol{r}, \boldsymbol{r}')|_{r'=\alpha+} \tag{17}$$

then the right-hand side of (15) is equal to zero and the following simple result is obtained:

$$p_\omega(\boldsymbol{r}) = \iiint_{v(r' < \alpha)} d\boldsymbol{r}' G_\omega(\boldsymbol{r}, \boldsymbol{r}') V_\omega(\boldsymbol{r}') \tag{18}$$

where the integration is carried out only over the spherical volume since $V_\omega(\boldsymbol{r}') = 0$ for $r' > \alpha$. The real pressure field $p(\boldsymbol{r}, t)$ is derived from (18) by computing the inverse Fourier transform with the aid of the convolution theorem:

$$p(\boldsymbol{r},t)=F^{-1}(p_\omega(\boldsymbol{r}))$$
$$=\iiint_{v} d\boldsymbol{r}' \int_{-\infty}^{+\infty} dt' G(\boldsymbol{r},\boldsymbol{r}'/t-t')V(\boldsymbol{r}',t'). \quad (19)$$

This shows that the key point in computing the $p(\boldsymbol{r},t)$ pressure field is to obtain the Green's function $G(\boldsymbol{r},\boldsymbol{r}'/t-t')$ satisfying the acoustic wave equation (10) and the boundary conditions (16) and (17) on the $r'=\alpha$ spherical surface. This subject is treated in the next section.

III. Dielectric Sphere Acoustic Green's Function

The source point $\boldsymbol{r}'$ (see (7) and (10)) being always inside the dielectric sphere, only the case when $r'<\alpha$ will be treated here. Then for $r<\alpha$, inside the dielectric sphere region, the Green's function can be split into two terms:

$$G_\omega(\boldsymbol{r},\boldsymbol{r}')=G_\omega^{(0)}(\boldsymbol{r},\boldsymbol{r}')+G_\omega^{(1)}(\boldsymbol{r},\boldsymbol{r}') \qquad (0<r<\alpha) \quad (20)$$

where $G_\omega^{(0)}(\boldsymbol{r},\boldsymbol{r}')$ is the solution of the inhomogeneous wave equation

$$(\nabla^2+\kappa_1^2)G_\omega^{(0)}(\boldsymbol{r},\boldsymbol{r}')=-\delta(\boldsymbol{r}-\boldsymbol{r}') \quad (21)$$

with $\kappa_1=\omega/c_1$ and $0<r<+\infty$. Notice that $G_\omega^{(0)}(\boldsymbol{r},\boldsymbol{r}')$ is the free-space acoustic Green's function. The second term in (20) is needed to satisfy the appropriate boundary conditions given in (16) and (17) and can be interpreted as the reaction of the surface discontinuity at $r=\alpha$. It is evident from (10) and (21) that

$$(\nabla^2+\kappa_1^2)G_\omega^{(1)}(\boldsymbol{r},\boldsymbol{r}')=0 \qquad (0<r<\alpha). \quad (22)$$

In the region $r>\alpha$, outside of the sphere,

$$G_\omega(\boldsymbol{r},\boldsymbol{r}')=G_\omega^{(2)}(\boldsymbol{r},\boldsymbol{r}')$$

and

$$(\nabla^2+\kappa_2^2)G_\omega^{(2)}(\boldsymbol{r},\boldsymbol{r}')=0 \quad (23)$$

where $\kappa_2=\omega/c_2$ and $G_\omega^{(2)}(\boldsymbol{r},\boldsymbol{r}')$ should satisfy the radiation conditions for $r\to+\infty$.

The solution of (21) is well known and can be written either in a closed form or as an expansion into spherical waves [15] (both given here):

$$G^{(0)}(\boldsymbol{r},\boldsymbol{r}')=\frac{e^{-j\kappa_1|\boldsymbol{r}-\boldsymbol{r}'|}}{4\pi|\boldsymbol{r}-\boldsymbol{r}'|}$$
$$=-\frac{j\kappa_1}{4\pi}\sum_{n=0}^{+\infty}\sum_{m=0}^{n}\epsilon_m(2n+1)\cdot\frac{(n-m)!}{(n+m)!}j_n(\kappa_1 r_<)h_n^{(2)}(\kappa_1 r_>)\cdot P_n^m(\cos\theta)P_n^m(\cos\theta')\cos(m(\varphi-\varphi')) \quad (24)$$

where (r,θ,φ) and (r',θ',φ') are the spherical coordinates of the observation $\boldsymbol{r}$ and source $\boldsymbol{r}'$ points, respectively. The $j_n(\cdot)$ and $h_n^{(2)}(\cdot)$ are the spherical Bessel and Hankel (second kind) functions, respectively, and $P_n^m(\cdot)$ is the associated Legendere polynomial of nth degree and mth order.

The notation $r_<$ and $r_>$ used in (24) is defined as follows:

$$r_<=\min(r,r')$$
$$r_>=\max(r,r').$$

Finally the coefficient ϵ_m is

$$\epsilon_m=\begin{cases}1 & \text{for } m=0\\ 2 & \text{for } m=1,2,\cdots.\end{cases}$$

The solutions of (22) and (23) can be written in terms of spherical waves in the following form:

$$G_\omega^{(1)}(\boldsymbol{r},\boldsymbol{r}')=-\frac{j\kappa_1}{4\pi}\sum_{n=0}^{+\infty}\sum_{m=0}^{n}\epsilon_m a_n(2n+1)\cdot\frac{(n-m)!}{(n+m)!}j_n(\kappa_1 r)j_n(\kappa_1 r')\cdot P_n^m(\cos\theta)P_n^m(\cos\theta')\cos(m(\varphi-\varphi')) \quad (25)$$

$$G_\omega^{(2)}(\boldsymbol{r},\boldsymbol{r}')=-\frac{j\kappa_2}{4\pi}\sum_{n=0}^{+\infty}\sum_{m=0}^{n}\epsilon_m b_n(2n+1)\cdot\frac{(n-m)!}{(n+m)!}h_n^{(2)}(\kappa_2 r)j_n(\kappa_1 r')\cdot P_n^m(\cos\theta)P_n^m(\cos\theta')\cos(m(\varphi-\varphi')). \quad (26)$$

Notice that the radial wave functions $j_n(\kappa,r)$ and $h_n^{(2)}(\kappa_2 r)$ are dictated by the requirement of a finite value of the field at $r=0$ and the radiation condition at $r\to+\infty$. In order to determine the unknown a_n and b_n coefficients, the boundary conditions given in (16) and (17) should be satisfied. Then employing the orthogonality properties of the $p_n^m(\cos\theta)$ and $\cos(m\varphi)$, $\sin(m\varphi)$ functions [15] and after a lengthy algebra, it is found that

$$a_n=\frac{h_n'^{(2)}(\kappa_1\alpha)h_n^{(2)}(\kappa_2\alpha)\kappa_1\rho_{20}-h_n^{(2)}(\kappa_1\alpha)h_n'^{(2)}(\kappa_2\alpha)\rho_{10}\kappa_2}{h_n'^{(2)}(\kappa_2\alpha)j_n(\kappa_1\alpha)\kappa_2\rho_{10}-j_n'(\kappa_1\alpha)h_n^{(2)}(\kappa_2\alpha)\kappa_1\rho_{20}}. \quad (27)$$

The b_n expansion coefficient is not given here, since in the following analysis the $G_\omega^{(0)}$ and $G_\omega^{(1)}$ functions will be employed exclusively.

IV. Computation of the $p(r,t)$ Pressure Field for $r<a$

In order to determine the $p(r,t)$ pressure field inside the dielectric sphere given in (19), in addition to the Green's function $G(\boldsymbol{r},\boldsymbol{r}'/t-t')$, it is required to know the source term $V(\boldsymbol{r},t)$ defined in (6). Then it is necessary to compute the absorbed power per unit volume by using the well-known formula

$$\mathbb{P}(\boldsymbol{r},t)=\frac{\sigma}{2}\boldsymbol{E}(\boldsymbol{r})\cdot\boldsymbol{E}^*(\boldsymbol{r}) \quad (28)$$

where $\sigma=-\omega\epsilon_0\,\mathrm{Im}(\epsilon_r)$ is the electrical conductivity of the dielectric medium and $\boldsymbol{E}(\boldsymbol{r})$ is the complex (phasor) electric field inside the sphere $r<\alpha$. The $\boldsymbol{E}(\boldsymbol{r})$ can be computed easily by using the well-known Mie theory of scattering of a plane wave [16] from a dielectric sphere. To this end assume an incident plane wave propagating along the z axis and polarized linearly parallel to the x axis. Then the incident electric field is

$$E_{\text{inc}}(r) = \hat{x} U e^{-jk_0 z} e^{j\omega_0 t} \tag{29}$$

where U is the wave amplitude, ω_0 the electromagnetic field angular frequency, and $k_0 = \omega\sqrt{\epsilon_0 \mu_0}$ is the free-space propagation constant. Substituting into (28) the expression for the electric field as given by the Mie solution and rearranging the terms, it is found that

$$E(r)\cdot E^*(r) = |E(r)|^2 = \frac{U^2}{k_0^2|\epsilon_r|}\left(\cos^2\varphi F_1(r,\theta) + \sin^2 F_2(r,\theta)\right) \tag{30}$$

where the functions $F_1(r,\theta)$ and $F_2(r,\theta)$ are infinite series and their expressions are given in the Appendix. For pulsed microwave signals, in determining the $V(r,t)$ source function the envelope of the incident pulsed wave should be taken into account. If the pulse duration T_p is very large in comparison with the microwave signal period ($T_0 = 2\pi/\omega_0 \ll T_p$), the absorbed power per unit volume can be computed by multiplying (28) by the pulse envelope shape $\Pi(t/T_p)$. The ideal pulse envelope function $\Pi(x)$ is defined as follows:

$$\Pi(x) = \begin{cases} 1 & \text{for } 0 < x < 1 \\ 0 & \text{otherwise.} \end{cases} \tag{31}$$

Then the source function $V(r,t)$ by employing (6) can be written as follows:

$$V(r,t) = C_0 \frac{\sigma}{2}\frac{U^2}{k_0^2|\epsilon_r|}\left(\cos^2\varphi F_1(r,\theta) + \sin^2\varphi F_2(r,\theta)\right)\left(\delta(t) - \delta(t - T_p)\right) \tag{32}$$

where the derivative of the unit step function is used twice.

A. Free-Space Term Contribution $p_0(r,t)$

Following (24) and the definition of the inverse Fourier transform (13),

$$G^{(0)}(r, r'/t-t') = \frac{1}{8\pi^2}\int_{-\infty}^{+\infty} d\omega \frac{\exp\left(j\omega\left(t - t' - \frac{|r-r'|}{c_1}\right)\right)}{|r-r'|} = \frac{\delta\left(t - t' - \frac{|r-r'|}{c_1}\right)}{4\pi|r-r'|}. \tag{33}$$

Then on substituting (32) and (33) into (19) it is found that

$$P_0(r,t) = Q_0 \iiint_{v(r'<\alpha)} dr' \frac{\left(\cos^2\varphi F_1(r,\theta) + \sin^2\varphi F_2(r,\theta)\right)}{4\pi|r-r'|} \cdot \left(\delta\left(t - \frac{|r-r'|}{c_1}\right) - \delta\left(t - T_p - \frac{|r-r'|}{c_1}\right)\right) \tag{34}$$

where

$$Q_0 = \frac{C_0 \sigma u^2}{2k_0^2|\epsilon_r|}.$$

The integrals in (34), because of the $\delta(\cdot)$ functions appearing under the integral sign, can be reduced to two-dimensional integrals. Indeed, by choosing as an origin the specific observation point $r' = r$ and remembering that only the points $|r'| < \alpha$ should be taken into account, the three-dimensional integral in (34) is reduced to surface integrals to be computed over two spherical or spherical cap surfaces. These two surfaces correspond to the geometric loci defined by conditions (35) and (36), respectively, and are illustrated in Fig. 2. Of course the additional condition $|r'| < \alpha$ should also be satisfied. Therefore, it is evident that for sufficiently large $t \gg T_p$, $P_0(r,t) = 0$ and there is no contribution from the $G_\omega^{(0)}(r/r')$ term. This shows that the rising edge of the pulse at $t = 0$ will excite an acoustic phenomenon starting at $t = 0$ and lasting until $t = t_M = (\alpha + |r|)/c_1$ while the corresponding time period for the falling edge will be from $t = T_p$ to $t = t_M + T_p$. In Fig. 2 the surfaces contributing to the $p_0(r,t)$ pressure field are illustrated at different characteristic time instants. Therefore, instead of (34), the $p_0(r,t)$ field is computed from

$$P_0(r,t) = \frac{Q_0}{4\pi}\left[c_1 t \iint_{s_\uparrow} ds' \Phi(\theta', \varphi', r')\Big|_{|r-r'|=c_1 t} \Pi(t/T_p) - c_1(t - T_p)\iint_{s_\downarrow} ds'\Phi(\theta',\varphi',r')\Big|_{|r-r'|=c_1(t-T_p)} \cdot \Pi\left((t-T_p)/T_p\right)\right] \tag{35}$$

where

$$\Phi(\theta', \varphi', r') = \cos^2\varphi' F_1(r', \theta') + \sin^2\varphi' F_2(r', \theta')$$

and the $s_\uparrow$ and $s_\downarrow$ surfaces are defined in Fig. 2.

B. Cavity Mode Contributions $P_l(r,t)$

On substituting (32) into (19), inserting for $G(r, r'/t-t') = G^{(1)}(r, r'/t-t')$, and introducing the inverse Fourier transformation given in (13), it is found that

$$p_1(r,t) = \frac{Q_0}{2\pi}\iiint_{(r'<\alpha)} dr' \int_{-\infty}^{+\infty} d\omega \cdot \left(e^{j\omega t}u(t) - e^{j\omega(t-T_p)}u(t-T_p)\right) \cdot G_\omega^{(1)}(r, r')\left(\cos^2\varphi' F_1(r',\theta') + \sin^2\varphi' F_2(r',\theta')\right). \tag{36}$$

The expression for $G_\omega^{(1)}(r, r')$ has already been determined and is given by (25) and (27). To this end substituting (25) into (36), the integration over the φ' variables can be performed easily. Furthermore the integral for the ω variable can be determined by using contour integration the-

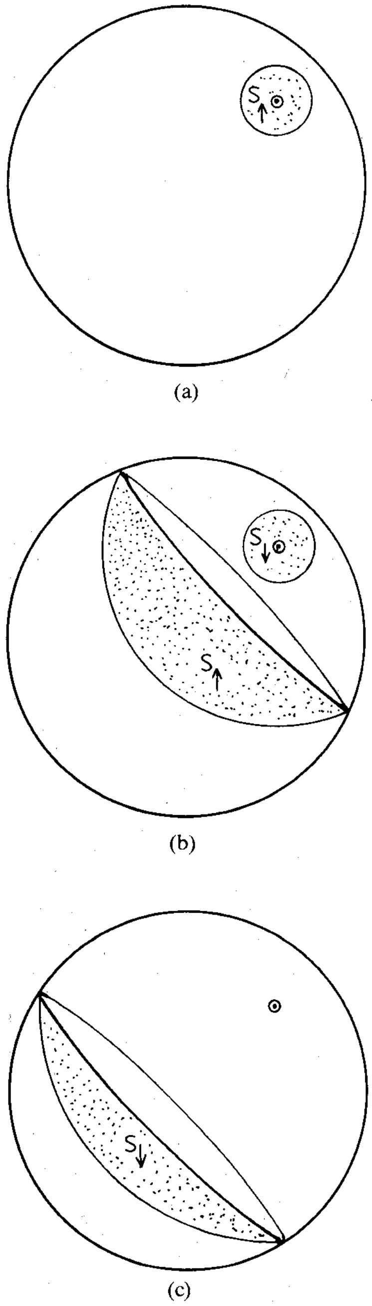

Fig. 2. Spherical surfaces $S_{\uparrow}$ and $S_{\downarrow}$ showing the contributions to the $p_0(\boldsymbol{r}, t)$ field at three different instants. Assuming the microwave pulse starts at $t=0$ and lasts until $t=T_p$, the three cases are (a) $0<t<T_p$; (b) $T_p<t<t_M$; and (c) $t_M<t<t_M+T_p$.

ory. Examination of the $a_n = a_n(\omega)$ dependence to the ω complex variable shows that there are an infinite number of poles corresponding to the roots of the equation

$$j_n\left(\frac{\omega}{c_1}\alpha\right) = \Delta_\epsilon A_n(\omega) \tag{37}$$

where

$$\Delta_\epsilon = \frac{c_2}{c_1}\frac{\rho_{20}}{\rho_{10}} \tag{38}$$

and

$$A_n(\omega) = \frac{j_n'\left(\frac{\omega\alpha}{c_1}\right) h_n^{(2)}\left(\frac{\omega\alpha}{c_2}\right)}{h_n'^{(2)}\left(\frac{\omega\alpha}{c_2}\right)}. \tag{39}$$

Notice that when the external dielectric medium is air, because $\rho_{20} \ll \rho_{10}$ and $c_2 < c_1$, the right-hand side of (37) is a perturbation term. Therefore an iterative procedure starting from the zeroth-order solution

$$j_n\left(\frac{\omega_{nl}\alpha}{c_1}\right) = 0 \tag{40}$$

can be employed. The integer $l = 1, 2, \cdots$ denotes the order of the root for a specific integer n. When $\Delta_\epsilon \neq 0$, the roots of (37) are complex numbers and always $\operatorname{Im}(\omega_{nl}) > 0$. Furthermore it can easily be shown that if $\omega = \omega_{nl}$ is a root of (37), then $\omega = -\omega_{nl}^*$ is also a root. The integrand function of (36) vanishes when $|\omega| \to +\infty$ and $\operatorname{Im}(\omega) > 0$. Therefore a complex contour integration procedure can be applied to compute the integral over the ω variable, leading to the result

$$\begin{aligned} p_1(\boldsymbol{r}, t) = \frac{Q_0}{2c_1} \sum_{n=0}^{\infty} (2n+1) \int_{r'=0}^{\alpha} \int_{\theta=0}^{\pi} dr'\, d\theta' r'^2 \sin\theta' \\ \cdot \Bigg\{ P_n^{(0)}(\cos\theta) P_n^{(0)}(\cos\theta') \left(F_1(r', \theta') + F_2(r', \theta')\right) \\ + \frac{(n-2)!}{(n+2)!} P_n^{(2)}(\cos\theta) P_n^{(2)}(\cos\theta') \\ \cdot \left(F_1(r', \theta') - F_2(r', \theta')\right) \cos 2\varphi \Bigg\} \\ \cdot \sum_{l=0}^{\infty} \operatorname{Re}\left(\frac{p(\omega_{nl}, t)}{\left.\frac{\partial Q(\omega)}{\partial\omega}\right|_{\omega=\omega_{nl}}} \right) \end{aligned} \tag{41}$$

where

$$\begin{aligned} p(\omega, t) = -\omega j_n\left(\frac{\omega r}{c_1}\right) j_n\left(\frac{\omega r'}{c_1}\right) \\ \cdot \left(e^{j\omega t}u(t) - e^{j\omega(t-T_p)}u(t-T_p)\right) \\ \cdot \left(h_n^{(2)}\left(\frac{\omega\alpha}{c_1}\right) - \Delta_\epsilon \frac{h_n^{(2)}\left(\frac{\omega\alpha}{c_2}\right) h_n'^{(2)}\left(\frac{\omega\alpha}{c_1}\right)}{h_n'^{(2)}\left(\frac{\omega\alpha}{c_2}\right)} \right) \end{aligned} \tag{42}$$

$$\cdot Q(\omega) = j_n\left(\frac{\omega\alpha}{\rho_1}\right) - \Delta_\epsilon A_n(\omega). \tag{43}$$

V. Numerical Results and Discussion

Numerical computations have been performed by applying the analytical results given in (35) and (41) for the $p_0(\boldsymbol{r}, t)$ and $p_1(\boldsymbol{r}, t)$ contributions, respectively. In both cases, the two-dimensional integrals encountered are com-

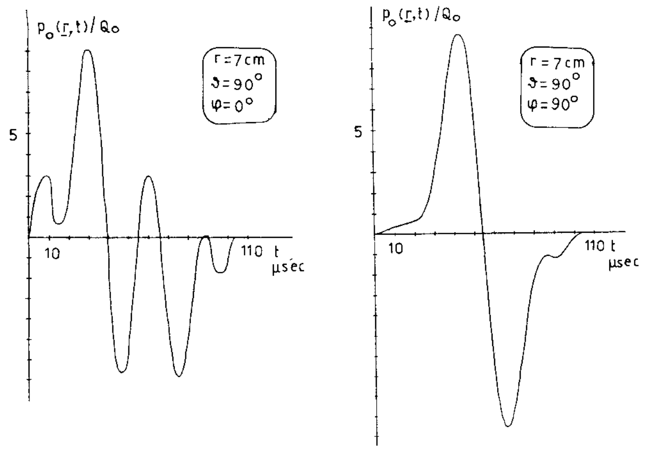

Fig. 3. Free-space $p_0(\boldsymbol{r},t)$ contribution pressure field variation with time at two points on the surface of the dielectric sphere.

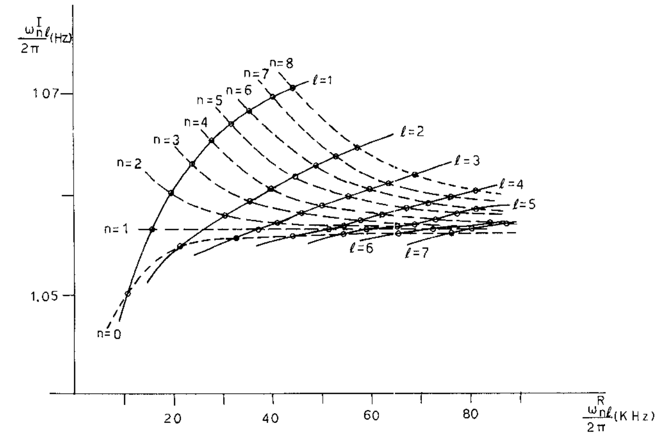

Fig. 4. Complex resonance frequencies for $c_1 = 1510$ m/s, $c_2 = 373$ m/s, and $\alpha = 7$ cm.

puted numerically by utilizing a multisegment 12 point Gaussian quadrature formula. Extensive convergence tests have been performed to ensure convergence.

The computations are carried for a dielectric sphere of $\alpha = 7$ cm radius, and the incident pulse carrier frequency is taken to be $(\omega_0/2\pi) = 432$ MHz with a $T_p = 10$ μs pulse width. The complex relative permittivity of the sphere is taken to be equal to that of water $\epsilon_r = 78 - j1.25$ at this frequency. The acoustic properties of the material and air media are defined in terms of the propagation frequencies $c_1 = 1510$ m/s and $c_2 = 373$ m/s, respectively. The proportionality constant C_0 in (1) is found to be [14] $C_0 = 2114.036$. Finally the average mass densities of the material and air media are taken to be $\rho_{10} \cong 10^3$ kg/m^3 and $\rho_{20} = 1.295$ kg/m^3, respectively.

In Fig. 3 the variation of the $p_0(\boldsymbol{r},t)$ free-space contribution is presented on the surface of the dielectric sphere at two different observation points. The transient phenomenon lasts 102.7 μs from the beginning of the microwave pulse. There is a significant difference between the two waveforms.

In order to determine the acoustic cavity mode contributions, the complex $\omega = \omega_{nl}$ $(n = 0,1,2,\cdots;\ l = 1,2,\cdots)$ roots of (37) should be determined in the first place. In Fig. 4 the spectra of the complex $\omega = \omega_{nl}$ resonance frequencies are presented on a complex plane. The lowest mode is found to be very close to the resonance frequency of the stress-free surface sphere, that is,

$$\omega_{01} \simeq \frac{\pi c_1}{\alpha} \tag{44}$$

which is in agreement with the predictions of Lin [17]. Furthermore if the lowest mode is considered separately, the corresponding damped wave packet from (41) and (42) is determined to be proportional to

$$e^{-\omega_{01}^I(t-T_p)}\Big[\Big(e^{-\omega_{01}^I T_p}\cos\varphi_{01} - \cos\big(\varphi_{01} - \omega_{01}^R T_p\big)\cos\omega_{01}^R t - \Big(e^{-\omega_{01}^I T_p}\sin\varphi_{01} - \sin\big(\varphi_{01} - \omega_{01}^R T_p\big)\Big)\sin\omega_{01}^R t\Big] \tag{45}$$

where $t > T_p$, $\omega_{01} = \omega_{01}^R + j\omega_{01}^I$, and φ_{01} is a phase constant. Then computing the amplitude of this waveform by applying standard trigonometry rules, it is found that the expression

$$e^{-\omega_{01}^I(t-T_p)}\Big[e^{-2\omega_{01}^I T_p} - 2\cos\big(\omega_{01}^R T_p\big)e^{-\omega_{01}^I T_p} + 1\Big]^{1/2} \tag{46}$$

determines the dependence of the wave amplitude on the incident pulse width. Therefore when $T_p \to 0$ the induced amplitude is zero. Provided that $\omega_{01}^I \ll \omega_{01}^R$, when $\omega_{01}^R T_p \approx \pi$ the dominant acoustic mode amplitude takes it peak value. If the acoustic losses were also incorporated in the analysis, then ω_{01}^I would be significantly larger than those presented in Fig. 4. In this case when $\omega_{01}^I T_p \gg 1$ the wave amplitude becomes independent of the pulse width T_p. Observe that in qualitative terms, the result present in (46) for the dependence of the dominant mode amplitude on the incident pulse width is in very good agreement with the experimental results obtained by Chou and Guy [3]. Notice that the incident microwave peak power hearing threshold is proportional to the inverse of the quantity given in (46). Therefore, for narrow incident pulses, higher peak powers are needed to cause acoustic sensation, while when T_p is sufficiently large the acoustic threshold is almost independent of the pulse width (see [3, table I]).

The pressure waveforms of the cavity mode contributions have been also computed by including all the significant mode amplitudes. In Fig. 5 the variation of the $p_1(\boldsymbol{r},t)$ pressure is presented at three specific points. The observed waveforms are very similar with those given in [13, fig. 3].

VI. Conclusions

The microwave-induced auditory effect in a dielectric sphere has been analyzed in detail. It is shown that an impinging pulse modulated microwave signal induces two types of pressure waves inside a dielectric sphere, namely a transient-type short-duration acoustic wave and a set of resonance modes belonging to the spherical acoustic resonator. The properties of these waves are investigated thoroughly.

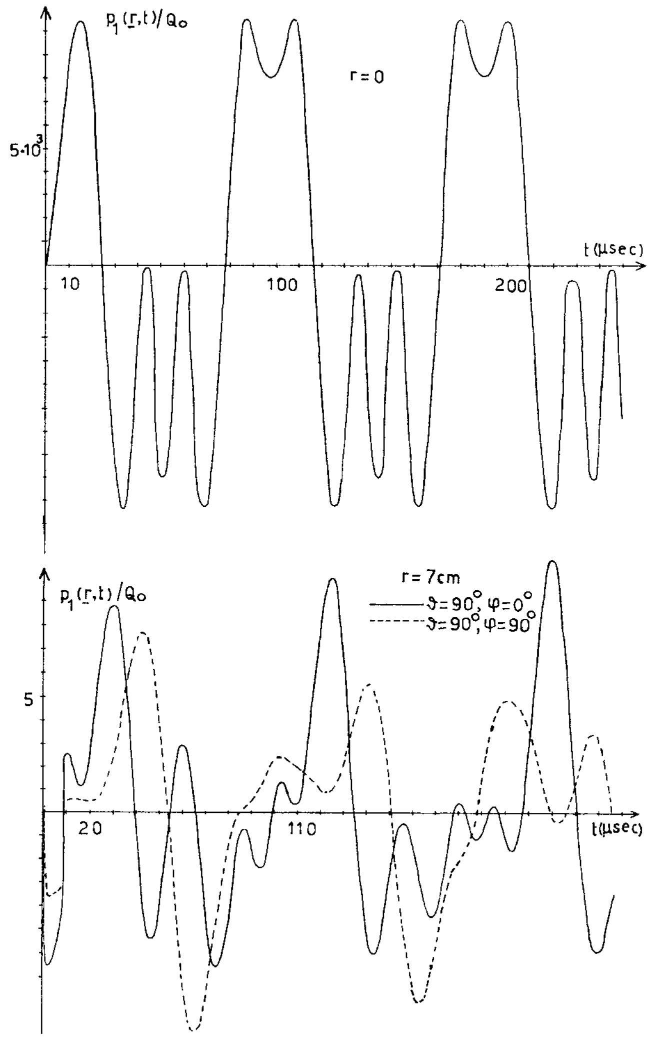

Fig. 5. Variation of the cavity mode $p_1(\boldsymbol{r}, t)$ contribution with time at three points of the dielectric sphere.

Appendix
Expressions for the $F_1(r,\theta)$ and $F_2(r,\theta)$ Functions

$$|\boldsymbol{E}(\boldsymbol{r})|^2 = \frac{U^2}{\kappa_0^2|\epsilon_r|}\left[\cos^2\varphi F_1(r,\theta) + \sin^2\varphi F_2(r,\theta)\right] \quad \text{(A1)}$$

$$F_1(r,\theta) = \left[\sum_{n=1}^{\infty} f_0(n) f_1(n,r,\theta)\right]^2 + \left[\sum_{n=1}^{\infty} f_0(n) f_2(n,r,\theta)\right]^2 \quad \text{(A2)}$$

$$F_2(r,\theta) = \left[\sum_{n=1}^{\infty} f_0(n) f_3(n,r,\theta)\right]^2 \quad \text{(A3)}$$

$$f_0(n) = (-j)^n \frac{2n+1}{n(n+1)} \quad \text{(A4)}$$

$$f_1(n,r,\theta) = c_n \frac{j_n(m\kappa r)}{r} P_n^1(\cos\theta)(n^2+n) \quad \text{(A5)}$$

$$f_2(n,r,\theta) = d_n \frac{P_n^1(\cos\theta)}{\sin\theta} j_n(m\kappa r) - c_n P_n^{1\prime}(\cos\theta)\sin\theta\left[m\kappa j_n'(m\kappa r) + \frac{j_n(m\kappa r)}{r}\right] \quad \text{(A6)}$$

$$f_3(n,r,\theta) = d_n P_n^{1\prime}(\cos\theta)\sin\theta j_n(m\kappa r) - c_n \frac{P_n^1(\cos\theta)}{\sin\theta}\left[m\kappa j_n'(m\kappa r) + \frac{j_n(m\kappa r)}{r}\right] \quad \text{(A7)}$$

$$c_n = m\frac{j_n(\kappa\alpha)\left[xh_n^{(2)}(x)\right]'_{\kappa\alpha} - h_n^{(2)}(\kappa\alpha)\left[xj_n(x)\right]'_{\kappa\alpha}}{\epsilon_r j_n(m\kappa\alpha)\left[xh^{(2)}(x)\right]'_{\kappa\alpha} - h_n^{(2)}(\kappa\alpha)\left[xj_n(x)\right]'_{\kappa\alpha}} \quad \text{(A8)}$$

$$d_n = \frac{\mu_r}{z_c}\frac{j_n(\kappa\alpha)\left[xh_n^{(2)}(x)\right]'_{\kappa\alpha} - h_n^{(2)}(\kappa\alpha)\left[xj_n(x)\right]'_{\kappa\alpha}}{\mu_r j_n(m\kappa\alpha)\left[xh_n^{(2)}(x)\right]_{\kappa\alpha} - h_n^{(2)}(\kappa\alpha)\left[xj_n(x)\right]'_{m\kappa\alpha}} \cdot(-j\omega\mu_0) \quad \text{(A9)}$$

$$z_c = (\mu_0/\epsilon_0\epsilon_r)^{1/2} \qquad m = (\epsilon_r)^{1/2} \quad \text{(A10)}$$

References

[1] A. H. Frey, "Auditory system response to radio-frequency energy," *Aerosp. Med.*, vol. 32, pp. 1140–1142, 1961.

[2] A. H. Frey and R. Messenger, Jr., "Human perception of illumination with pulsed ultra-high frequency electromagnetic energy," *Science*, vol. 181, pp. 356–358, 1973.

[3] C. K. Chou and A. W. Guy, "Microwave-induced auditory responses in guinea pigs: Relationship of threshold and microwave-pulse duration," *Radio Sci.*, vol. 14, pp. 193–197, 1979.

[4] J. C. Lin, R. J. Meltzer, and F. K. Redding, "Comparison of measured and predicted characteristics of microwave-induced sound," *Radio Sci.*, vol. 17, pp. 1595–1635, 1982.

[5] A. W. Guy, C. K. Chou, J. C. Lin, and D. Christensen, "Microwave induced acoustic effects in mammalian auditory system and physical materials," *Ann. N.Y. Acad. Sci.*, vol. 247, pp. 194–215, 1975.

[6] C. K. Chou, R. Galambos, A. W. Guy, and R. H. Lovely, "Cochlear microphonics generated by microwave pulse," *J. Microwave Power*, vol. 10, pp. 361–367, 1975.

[7] J. C. Lin, *Microwave Auditory Effects and Applications*. Springfield, IL: C. C. Thomas, 1978.

[8] H. C. Sommer and H. E. Von Gierke, "Hearing sensations in electric field," *Aerosp. Med.*, vol. 35, pp. 834–839, 1964.

[9] J. C. Sharp, H. M. Grove, and O. P. Gandhi, "Generation of acoustic signals by pulsed microwave energy," *IEEE Trans. Microwave Theory Tech.*, vol. MTT-22, pp. 583–584, 1974.

[10] K. R. Foster and E. D. Finch, "Microwave hearing: Evidence for thermoacoustical auditory stimulation by pulsed microwaves," *Science*, vol. 185, pp. 256–258, 1974.

[11] J. C. Lin, "Microwave auditory effect—A comparison of some possible transduction mechanisms," *J. Microwave Power*, vol. 11, pp. 77–81, 1976.

[12] J. C. Lin, "On microwave-induced hearing sensation," *IEEE Trans. Microwave Theory Tech.*, vol. MTT-25, pp. 605–613, 1977.

[13] J. C. Lin, "Further studies on the microwave auditory effect," *IEEE Trans. Microwave Theory Tech.*, vol. MTT-25, pp. 938–943, 1977.

[14] T. C. Guo, W. W. Guo, and L. E. Larsen, "Microwave-induced thermoacoustic effect in dielectrics and its coupling to external medium—A thermodynamical formulation," *IEEE Trans. Microwave Theory Tech.*, vol. MTT-32, pp. 835–843, 1984.

[15] P. Morse and H. Feshbach, *Methods of Theoretical Physics*, part II. New York: McGraw—Hill, 1953, pp. 1466–1467.

[16] G. Mie, *Ann.d. Physik* (*4*), vol. 25, p. 377, 1908.
[17] J. C. Lin, "The microwave auditory phenomenon," *Proc. IEEE*, vol. 68, pp. 67–73, 1980.

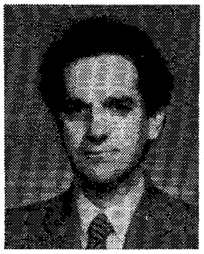

Nikolaos K. Uzunoglu (M'82) received the B.Sc. degree in electronics engineering from the Istanbul Technical University, Turkey, in 1973. He obtained the M.Sc. and Ph.D. degrees from the University of Essex, England, in 1974 and 1976, respectively.

He worked for the Hellenic Navy Research and Technology Development Office from 1977 to 1984. During this period, he also worked on a part-time basis at the national Technical University of Athens on electromagnetic theory. In 1984, he was elected Associate Professor at the National Technical University of Athens and in 1988 Professor at the same university, the position that he holds presently. He is Associate Dean of the Department of Electrical Engineering for the years 1986–1988. His research interests are microwave applications in telecommunications and medicine, fiber-optic components, and electromagnetic theory.

Spyridon I. Polychronopoulos received a degree in electrical engineering from the National Technical University of Athens in 1987. He is currently pursuing the M.Sc. degree in communication engineering and digital electronics at the University of Manchester Institute of Science and Technology. His research interests are in the areas of microwave circuits, radar systems, and biomedical applications of microwaves.